Epigenetic regulation of intestinal stem cells by Tet1-mediated DNA hydroxymethylation

Rinho Kim, Karyn L. Sheaffer, Inchan Choi, Kyoung-Jae Won, and Klaus H. Kaestner

Department of Genetics, Center for Molecular Studies in Digestive and Liver Diseases, Perelman School of Medicine, University of Pennsylvania, Philadelphia, Pennsylvania 19104, USA

Methylated cytosines are associated with gene silencing. The ten-eleven translocation (TET) hydroxylases, which oxidize methylated cytosines to 5-hydroxymethylcytosine (5hmC), are essential for cytosine demethylation. Gene silencing and activation are critical for intestinal stem cell (ISC) maintenance and differentiation, but the potential role of TET hydroxylases in these processes has not yet been examined. Here, we generated genome-wide maps of the 5hmC mark in ISCs and their differentiated progeny. Genes with high levels of hydroxymethylation in ISCs are strongly associated with Wnt signaling and developmental processes. We found Tet1 to be the most abundantly expressed Tet gene in ISCs; therefore, we analyzed intestinal development in *Tet1*-deficient mice and determined that these mice are growth-retarded, exhibit partial postnatal lethality, and have significantly reduced numbers of proliferative cells in the intestinal epithelium. In addition, the *Tet1*-deficient intestine displays reduced organoid-forming capacity. In the *Tet1*-deficient crypt, decreased expression of Wnt target genes such as *Axin2* and *Lgr5* correlates with lower 5hmC levels at their promoters. These data demonstrate that Tet1-mediated DNA hydroxymethylation plays a critical role in the epigenetic regulation of the Wnt pathway in intestinal stem and progenitor cells and consequently in the self-renewal of the intestinal epithelium.

[*Keywords*: Tet1; epigenomics; hydroxymethylation; intestinal differentiation; intestinal stem cell]

Supplemental material is available for this article.

Received July 28, 2016; revised version accepted October 21, 2016.

DNA methylation is a widespread epigenetic modification that regulates gene expression in development and cellular differentiation (Reik et al. 2001; Smith and Meissner 2013; Sheaffer et al. 2014). DNA methylation is dynamic yet tightly regulated to prevent aberrant patterns of 5-methylcytosine (5mC), which are common in cancer (Baylin et al. 2001; Esteller 2007). 5mC is established and maintained by DNA methyltransferase (DNMT) enzymes (Li et al. 1992; Okano et al. 1999). Recently, oxidation of 5mC to 5-hydroxymethylcytosine (5hmC) by the ten-eleven translocation (TET) gene family was proposed as a novel mechanism for removal of 5mC (Kriaucionis and Heintz 2009; Tahiliani et al. 2009). This can occur by at least two nonmutually exclusive mechanisms. First, 5hmC can be further oxidized to 5-formlyctosine (5fC) and then 5-carboxylcytosine (5caC), again by the Tet enzymes, although at much lower efficacy than oxidation from 5mC to 5hmC (Ito et al. 2011). Both 5fC and 5caC can be glycosylated by thymine DNA glycosylase and replaced by unmodified cytosine via base excision repair (Maiti and Drohat 2011; Weber et al. 2016). Second, because hemimethylated 5hmC nucleotides are not recognized by the maintenance DNA methyltransferases following DNA replication during S phase, hydroxymethylation of specific sites will lead to their targeted, passive demethylation in replicating cells. Thus, hydroxymethylation via the Tet enzymes offers an elegant pathway for even lineage-committed cells to change their DNA methylation status.

Global methylome analyses in recent years have shown that the DNA methylation status is dynamic with aging even within the same cell type (Avrahami et al. 2015). Likewise, we and others have demonstrated previously that DNA methylation at specific loci changes during differentiation of intestinal stem cells (ISCs) to enterocytes in adult mice (Kaaij et al. 2013; Sheaffer et al. 2014) and during ISC maturation in postnatal mice (Yu et al. 2015); however, how these elements are targeted for demethylation is currently unknown.

Corresponding author: kaestner@mail.med.upenn.edu
Article published online ahead of print. Article and publication date are online at http://www.genesdev.org/cgi/doi/10.1101/gad.288035.116.

The epithelium of the small intestine is the most rapidly self-renewing tissue in mammals, and, even in humans, the epithelium is replaced every 3–5 d. Active Wnt signaling in the intestinal crypt is a major driving force for ISC renewal and proliferation of transit-amplifying cells. Tight regulation of Wnt signaling is critical for the intestinal epithelial homeostasis (Gregorieff and Clevers 2005). Rapidly cycling Lgr5$^+$ stem cells at the bottom of the intestinal crypt give rise to transit-amplifying cells that divide up to six times further (Rao and Wang 2010) before differentiating into post-mitotic, functional cells as they exit the crypt zone and migrate up the crypt–villus axis. This process is accompanied by dramatic changes in the transcriptional program, which are mediated at least in part by epigenetic changes such as the aforementioned realignment of DNA methylation status (Kaaij et al. 2013; Sheaffer et al. 2014). In fact, in the absence of Dnmt1 alone or both Dnmt1 and Dnmt3b, the intestinal epithelium is not viable in the postnatal period (Yu et al. 2015) or in the adult (Elliott et al. 2016), respectively. Here, we investigate to what extent targeted oxidation of 5mC to 5hmC contributes to intestinal epithelial health.

Results

The 5hmC mark is prominent in intestinal villus epithelial cells

To determine global 5hmC levels in ISCs, we performed 5hmC dot blot analysis of genomic DNA from isolated epithelial cells as well as brain and embryonic stem cells (ESCs) for comparison. We found that 5hmC levels in the gut are almost as high as those present in the brain and ESCs (Fig. 1A). Hydroxymethylation of cytosines has been suggested to play an important role in neurons due to the abundance of this mark in the brain (Hahn et al. 2013; Rudenko et al. 2013). Therefore, we hypothesized that this epigenetic mark might also be critical for the proliferation and/or differentiation of intestinal epithelial cells. We examined the distribution of global 5hmC compared with 5mC in the intestinal epithelium by immunofluorescence detection of each mark with specific antibodies. 5mC was present in all epithelial cells, with the highest levels in the crypt, where stem and transit-amplifying cells reside (Fig. 1B). We identified proliferating stem and transit-amplifying cells by costaining with Ki67, a marker of proliferation. Interestingly, we found that the strongest 5hmC signal was detected in the nuclei of differentiated villus cells, while the signal decreased in the crypt region (Fig. 1C). This finding is consistent with previous reports that 5hmC is depleted in proliferating cancer cells compared with post-mitotic cells (Jin et al. 2011; Lian et al. 2012).

Dynamic changes of 5hmC distribution during intestinal epithelial differentiation

Next, we examined dynamic genomic 5hmC abundance during ISC differentiation. First, we isolated Lgr5-expressing ISCs (Lgr5$^+$) from Lgr5-EGFP–IRES-CreERT2 mice (Barker et al. 2007) by FACS and differentiated villus epithelial cells by careful scraping of the luminal side of the gut tube, respectively (Fig. 1D,E; see the detailed description in the Materials and Methods). Genomic DNA was then isolated from both cell populations. To investigate genome-wide changes of the 5hmC mark between Lgr5$^+$ and differentiated cells, we performed hydroxymethylated DNA immunoprecipitation (hMeDIP) followed by next-generation sequencing (hMeDIP-seq) (see the Materials and Methods). Remarkably, we discovered striking differences in 5hmC levels in marker genes for both ISCs and mature enterocytes (Fig. 2A–C). For example, high levels of 5hmC were present near promoters and throughout the gene bodies of ISC marker genes such as *Lgr5*, *Olfm4*, and *Msi1* and Wnt target genes such as *Axin2*, *c-Myc*, and *Sox9* in Lgr5$^+$ cells but were decreased dramatically after differentiation into villus epithelial cells (Fig. 2A,B). Conversely, genes expressed at high levels only in differentiated cells, such as *Alpi*, *Sis*, and *Fabp1*, were hydroxymethylated only in differentiated cells (Fig. 2C).

Having established that the 5hmC mark is dynamic for the nine genes described above, we performed a genome-wide analysis of hydroxymethylation. We found an approximately eightfold increase in the total 5hmC signal in differentiated cells relative to Lgr5$^+$ cells (Fig. 2D) and identified a total of 33,183 5hmC-enriched regions (peaks) in Lgr5$^+$ cells and 100,707 peaks in differentiated cells using HOMER (Fig. 2E; Heinz et al. 2010). When comparing 5hmC peaks between the two cell populations, we identified 10,450 differentially hydroxymethylated regions (DhMRs; fivefold or more; $P < 0.0001$) and divided them into two groups: higher 5hmC levels in Lgr5$^+$ cells ($n = 2537$) and higher 5hmC levels in differentiated cells ($n = 7903$) (Fig. 2F). Interestingly, the two groups of DhMRs displayed distinct genomic distribution patterns. While Lgr5$^+$ DhMRs were enriched in intergenic regions, those present in differentiated cells were more likely to be located in gene bodies. We identified the closest gene for each DhMR and performed gene ontology analysis for the differentially hydroxymethylated gene sets (Fig. 2G). The genes associated with higher 5hmC levels in Lgr5$^+$ cells were involved in "developmental process" and "cell differentiation," primary functions of stem cells. Conversely, the genes associated with higher 5hmC levels in differentiated cells were enriched for genes that control metabolic processes and nutrient transport, major functions of enterocytes. Thus, overall, high levels of hydroxymethylation correlated positively with the gene sets expected to be active in either Lgr5$^+$ stem cells or post-mitotic differentiated villus epithelial cells.

Next, we examined the correlation between differential hydroxymethylation and differential gene expression, determined by RNA sequencing (RNA-seq) (Sheaffer et al. 2014). Genes enriched for the 5hmC mark in Lgr5$^+$ stem cells—including ISC marker genes such as *Olfm4*, *Lgr5*, and *Msi1* and Wnt target genes such as *Axin2*, *c-Myc*, and *Sox9*—showed higher gene expression level in Lgr5$^+$ stem cells than in differentiated villus epithelial cells

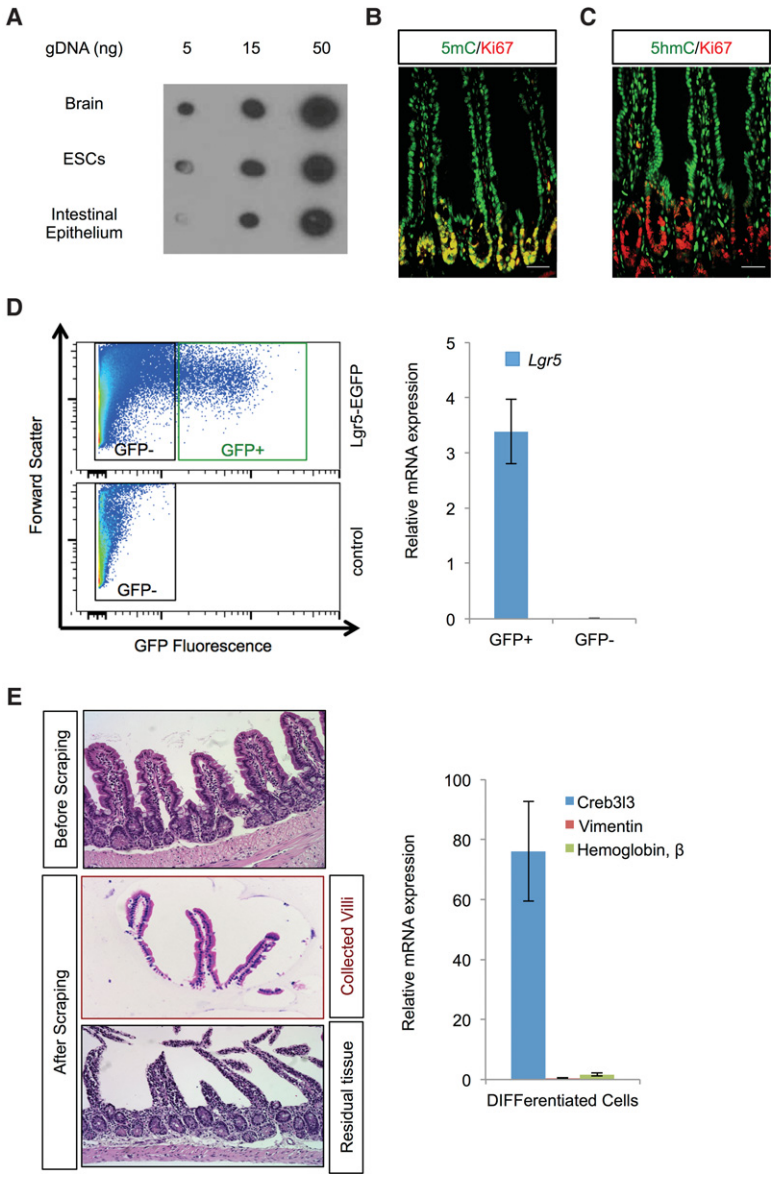

Figure 1. Differential 5hmC distribution in intestinal stem and differentiated cells. (*A*) The dot blot shows global 5hmC levels in the mouse adult intestinal epithelium compared with the brain and ESCs. (*B*, *C*) Immunofluorescence staining of mouse jejunum with 5mC (*B*), 5hmC (*C*), and Ki67 antibodies, as indicated. Bars, 50 µm. (*D*) FACS plot to isolate Lgr5-EGFP$^+$ cells and RT-qPCR validation for Lgr5 expression in GFP$^+$ cells. (*E*) H&E staining image of scraped differentiated villus cells and RT-qPCR validation for cell-specific marker genes. (Creb3l3) Enterocyte; (vimentin) mesenchymal cells; (hemoglobin) red blood cells.

(Fig. 3A,B). Conversely, genes enriched for the 5hmC mark in differentiated cells, including marker genes such as *Alpi*, *Sis*, and *Fabp1*, exhibited increased expression in differentiated cells (Fig. 3C). Overall, gene expression changes correlated strongly with 5hmC level variation during ISC differentiation (Fig. 3D,E). However, we also noted some exceptions where gene expression levels were anti-correlated with 5hmC status. 5hmC has been reported to have a role in transcriptional repression in specific cases, including poised enhancers (Pastor et al. 2011; Wu et al. 2011; Choi et al. 2014).

Tet1 is required for postnatal intestinal development

Having determined that hydroxymethylation is highly dynamic during differentiation of ISCs into functional villus epithelial cells, we investigated which of the Tet enzymes is most likely controlling this process. We determined Tet1, Tet2, and Tet3 mRNA expression levels in Lgr5$^+$ stem cells and differentiated villus cells by quantitative RT–PCR (qRT–PCR) (Fig. 4A). *Tet1* was expressed at much higher levels in Lgr5$^+$ stem cells than in differentiated cells, while *Tet2* and *Tet3* showed the opposite pattern. These data suggested that Tet1 might have an essential role in Lgr5$^+$ ISC function. Next, we phenotyped *Tet1*-null mutant mice (Dawlaty et al. 2011) during postnatal development, when gastrointestinal function first becomes relevant (Supplemental Table S1). Strikingly, we found that *Tet1*-deficient mice were growth-retarded during the early postnatal period (Fig. 4B) and showed significant postnatal lethality (Fig. 4C). In fact, viability of *Tet1*$^{-/-}$ mice was already significantly impaired by postnatal day 3 (P3) (Fig. 4D). Tet1-deficient mice exhibited a much smaller body size (Fig. 4E), and their intestines were shorter than those of wild-type littermates (Fig. 4F).

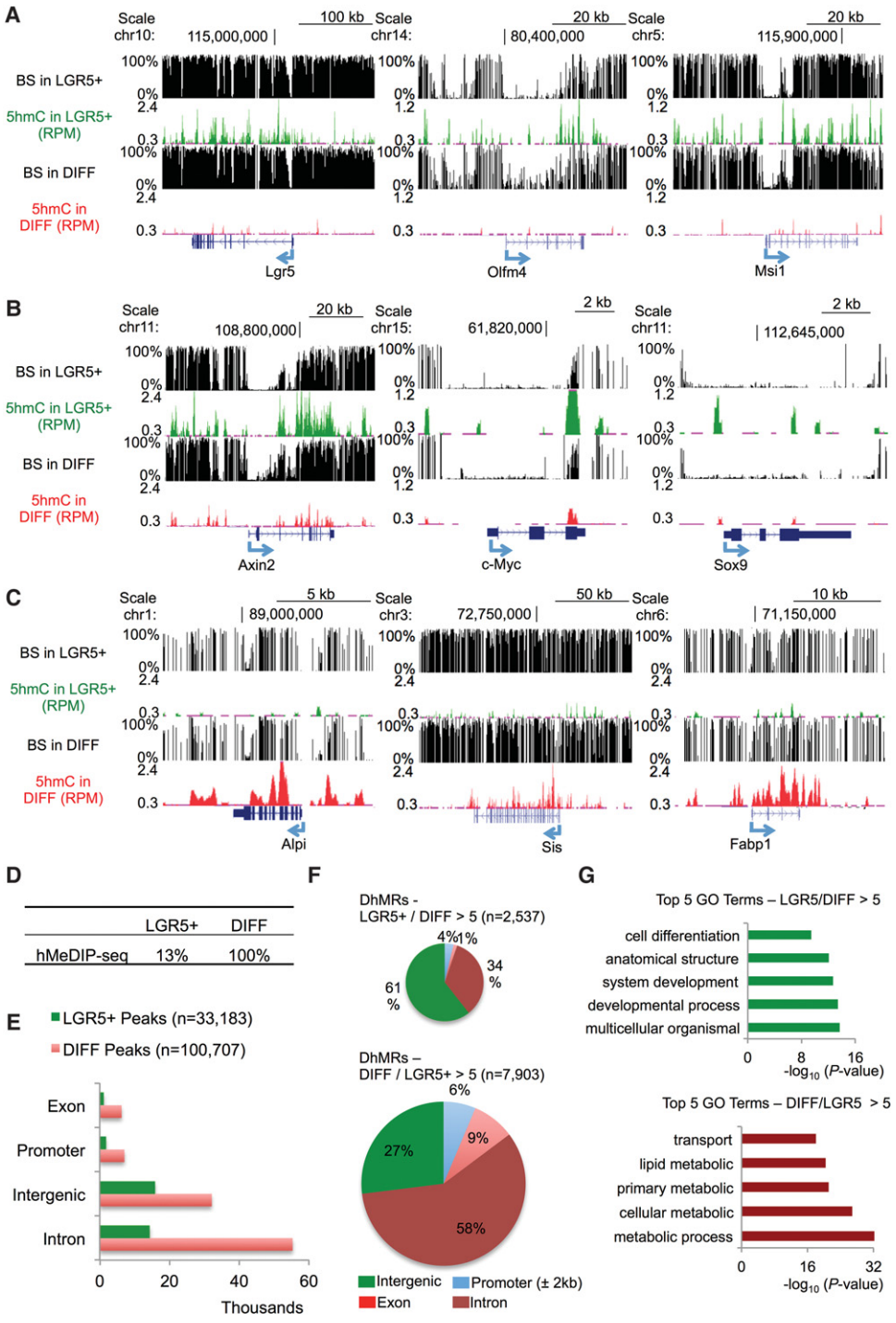

Figure 2. Genome-wide distribution of 5hmC and its dynamics. (*A–C*) Screenshots of bisulfite sequencing (which measures the sum of 5mC and 5hmC) and hMeDIP-seq (which determines 5hmC abundance only) at marker genes in Lgr5$^+$ ISCs (*A*), Wnt target genes (*B*), and marker genes of differentiated villus cells (*C*). Data are presented as percent methylation for the bisulfite sequencing data and as reads per million mapped reads (RPM) for the 5hmC data. (*D*) The relative 5hmC signal of hMedIP-seq in Lgr5$^+$ stem and differentiated cells. The ratio of hMeDIP/input reads numbers in differentiated epithelial cells (DIFF) was set to 100%. (*E*) The total number of 5hmC-enriched regions (peaks) and genomic distribution in Lgr5$^+$ stem and differentiated cells (fourfold or more enrichment over local tag count). *P*-value < 0.001. (*F*) Genomic distribution of differentially hydroxymethylated regions (DhMRs). (*Top* pie chart) regions with 5hmC levels that are higher in Lgr5$^+$ stem cells than in differentiated epithelial cells (DIFF) (at least fivefold). *P*-value < 0.0001. (*Bottom* pie chart) Regions with 5hmC levels that are higher in differentiated epithelial cells (DIFF) than in Lgr5$^+$ stem cells (at least fivefold). *P*-value < 0.0001. Circle size represents the total number of DhMRs in each group. (*G*) Gene ontology search results for genes closest to DhMRs.

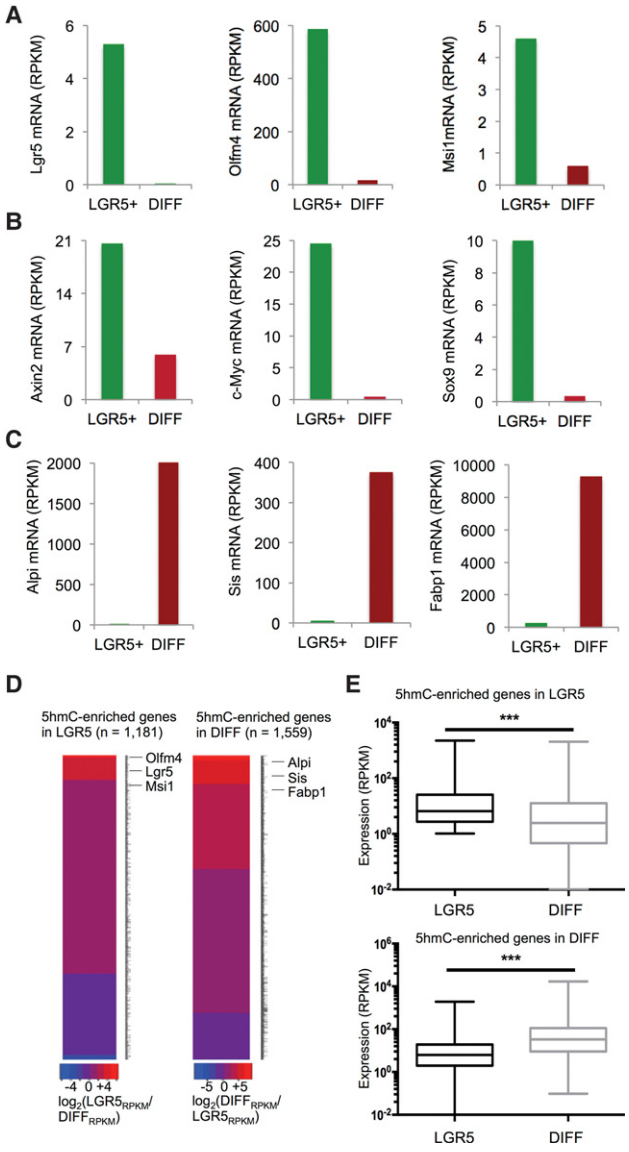

Figure 3. Positive correlation between 5hmC-enriched gene expression levels. (*A–C*) RNA-seq results for ISC marker genes (*A*), Wnt target genes (*B*), and differentiated villus cell marker genes (*C*). RNA-seq data for both cell populations are represented as reads per kilobase per million mapped read (RPKM). (*D*) Heat map for differential gene expression of differentially hydroxymethylated genes (≥1.5-fold change) during intestinal epithelial differentiation. (*E*) Box plot for differential gene expression of differentially hydroxymethylated genes in each cell population. (***) *P*-value < 0.001 by *t*-test.

Wnt target genes and Lgr5 expression in the postnatal intestine are dependent on Tet1 function

On histological examination, we found both villus length and proliferating cell number per crypt to be significantly reduced in *Tet1*-null mice compared with wild-type littermate controls (Fig. 5*A–C*). Thus, Tet1 plays an important role in the maturation of the postnatal intestine. Since Wnt signaling is essential for intestinal maturation and proliferation, we reasoned that Wnt target gene expression might be affected in *Tet1*-deleted mice. To examine Wnt target gene expression levels, we performed immunostaining for protein markers of Wnt pathway activation in 1-wk-old $Tet1^{-/-}$ jejunum compared with wild-type littermate controls. Expression of the Wnt target genes Axin2, c-Myc, and Sox9 was clearly reduced in the mutant small intestinal crypts (Fig. 5D).

To evaluate the consequences of *Tet1* deficiency on ISC maintenance, we crossed *Tet1* mutant with Lgr5-EGFP–IRES-CreERT2 mice, which allowed for the easy detection of $Lgr5^{+}$ stem cells via expression of EGFP. We found a dramatic reduction in the frequency of Lgr5-EGFP-positive cells in the crypt of the postnatal and adult *Tet1*-null jejunum (Fig. 6A–C). Thus, Tet1 is required for maintaining Wnt target gene expression and normal epithelial cell morphology in the intestinal crypt.

Decreased 5hmC levels at Wnt target loci lead to impaired organoid formation

Next, we investigated stem cell function in organoid culture. We found much smaller organoid size and significantly decreased organoid budding in cultures derived from the *Tet1*-deficient intestine (Fig. 7A–C). This suggests that the state of postnatal crypts from $Tet1^{-/-}$ mice is closer to fetal than adult crypts (Fordham et al. 2013; Mustata et al. 2013).

To ascertain whether the decrease in Wnt target genes and *Lgr5* expression in $Tet1^{-/-}$ mice was caused by altered methylation and hydroxymethylation levels, we analyzed 5mC and 5hmC levels at their loci in control and mutant mice. We found significantly increased 5mC levels at the *Axin2* and *Sox9* promoters and significantly decreased 5hmC levels at the promoters of *Lgr5*, *Axin2*, and *Sox9* in *Tet1*-null mice (Fig. 7D), which correlated with the decreased expression of these genes (Figs. 5D, 6A). These findings demonstrate that Tet1-mediated hydroxymethylation is critical to allow for full activation of Wnt target genes in intestinal crypts.

Discussion

In this study, we document dynamic changes of 5hmC at key gene loci during ISC differentiation and report that Tet1-mediated hydroxymethylation is essential for ISC function. 5hmC was enriched at promoters and gene bodies of highly expressed genes in each cell type and may reverse the repressive effect of 5mC for gene activation. Tet1 was expressed in ISCs but not in differentiated villus cells.

$Tet1^{-/-}$ mice on a mixed genetic background (129Sv and C57BL/6) were reported previously to be viable but had a smaller body size and lower body weight than wild-type animals at their postnatal age (Dawlaty et al. 2011; Zhang et al. 2013). Adult Tet1 mutant mice exhibited defective self-renewal of neural progenitor (Rudenko et al. 2013; Zhang et al. 2013; Xin et al. 2015) and hematopoietic stem (Cimmino et al. 2015) cells. However, after backcrossing onto the C57BL/6 background, we observed growth retardation and decreased postnatal viability in

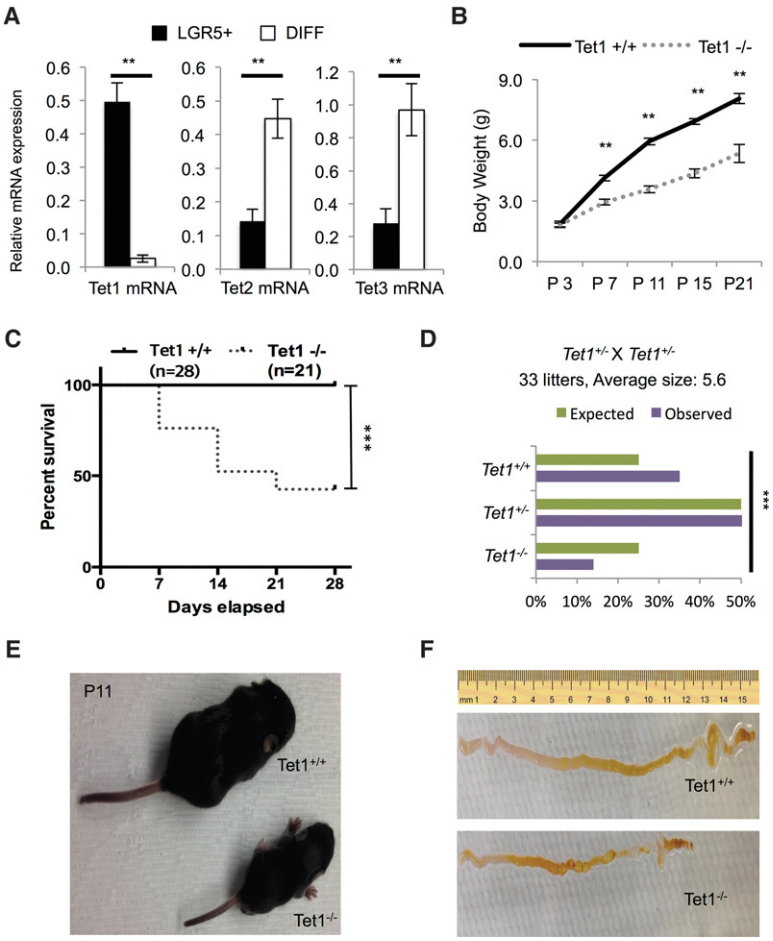

Figure 4. Postnatal developmental defects in the intestines of Tet1-null mice. (*A*) Relative Tet1/2/3 mRNA expression levels in Lgr5$^+$ intestinal stem and differentiated epithelial cells of adult mice. mRNA levels were normalized to those of *Tbp*. (*B*) Tet1-null mice are growth-retarded. Weight curve during the postnatal period. (**) *P*-value < 0.01 by *t*-test. (*C*) Survival curve during the postnatal period. (***) *P*-value < 0.001 by a log rank (Mantel-Cox) test. (*D*) Reduced perinatal viability of Tet1 homozygous mutants. Mice were quantified on P3. (***) *P*-value <0.0005, χ^2 test. (*E*) Representative *Tet1*$^{+/+}$ and *Tet1*$^{-/-}$ mice on P11. (*F*) Representative images of intestinal tracts of *Tet1*$^{+/+}$ and *Tet1*$^{-/-}$ mice at 1 wk of age.

these mice. Recently, Kang et al. (2015) also reported that *Tet1*-deficient C57BL/6 mice exhibit partial embryonic lethality and growth retardation; however, intestinal health was not examined in the prior study. *Tet1*$^{-/-}$ mice exhibited shortened intestinal length and reduced proliferating cell number in the postnatal intestine, which is similar to the phenotype seen in mice with conditional deletion of Dnmt1 in the developing gut using Dnmt1$^{f/f}$; VillinCre mice (Elliott et al. 2015; Yu et al. 2015).

Lgr5 is a Wnt target gene and a stem cell marker gene in the adult intestine (Barker et al. 2007); however, a limited number of Lgr5$^+$ cells are also present in the intervillus zone of the developing gut at embryonic day 16.5 (E16.5) (Kinzel et al. 2014). During intestinal maturation in the postnatal period, these Lgr5$^+$ cells are rapidly cycling at the bottom of the crypt and clearly exhibit stem cell properties at this stage (Kim et al. 2012). These data demonstrate that Lgr5 expression in ISCs is activated around birth and maintained throughout adult life. Here we show that 5hmC enrichment at Wnt target loci in Lgr5$^+$ stem cells is required for full activation of gene expression, and homozygous deletion of *Tet1* causes significantly decreased 5hmC levels at these loci, resulting in a dramatically reduced Wnt target gene expression. Importantly, loss of Tet1 also impairs budding organoid-forming capacity and thus de novo formation or expansion of stem cells in crypt culture. It was reported previously (Mustata et al. 2013) that when organoids are grown from the fetal intestine, they form spheroids instead of budding organoids and exhibit low levels of Wnt target gene expression. The organoids that we obtained from the Tet1-deleted postnatal intestine resemble these spheroids, suggesting an underdeveloped state.

In sum, our data demonstrate that Tet1-mediated conversion from 5mC to 5hmC is an important epigenetic mechanism regulating expression of Wnt target genes, including *Lgr5*, during postnatal intestinal maturation. The definitive role of Tet1-mediated DNA hydroxymethylation in the intestine warrants further investigation using conditional gene ablation models. Nevertheless, our results demonstrate that 5hmC is an essential epigenetic mark required for ISC function. DNA hydroxymethylation represents one of the switches required to activate key genes in postnatal crypt maturation and is a novel mechanism of gene regulation during ISC differentiation.

Materials and methods

Mice

All procedures involving mice were conducted under a protocol approved by the Institutional Animal Care and Use Committee

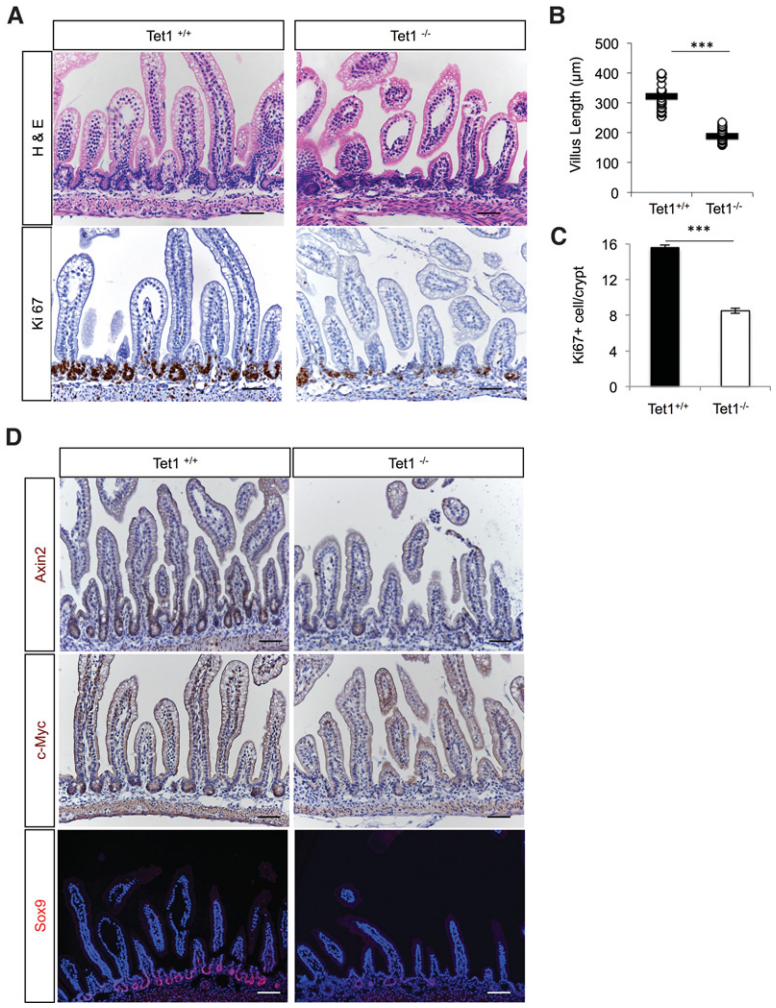

Figure 5. Decreased Wnt target gene expression in the postnatal *Tet1*-null intestine. (*A*) Histological analysis of $Tet1^{+/+}$ and $Tet1^{-/-}$ jejunum of 1-wk-old mice. Proliferating cells are marked by immunohistochemistry for Ki67 (dark-brown signal). Bars, 50 µm. (*B*) Villus length in $Tet1^{+/+}$ and $Tet1^{-/-}$ 1-wk-old jejunum. (***) *P*-value < 0.001. (*C*) $Ki67^{+}$ cell number per crypt is reduced in 1-wk-old $Tet1^{-/-}$ jejunum compared with littermate controls. (***) *P*-value < 0.001. (*D*) Immunostaining results of Wnt target gene expression, including Axin2, c-Myc, and Sox9 in P7 $Tet1^{+/+}$ and $Tet1^{-/-}$ mice. Bars, 50 µm.

(IACUC) of the University of Pennsylvania. C57BL/6J mice (8–12 wk old) were used for all experiments unless noted otherwise. For sorting of $Lgr5^{+}$ stem cells, we used *Lgr5-EGFP–Ires-CreERT2* mice (Barker et al. 2007). $Tet1^{-/-}$ mice (Dawlaty et al. 2011) were backcrossed to C57BL/6J mice for five generations. Eight-week-old $Tet1^{+/-}$ mice were then intercrossed to generate $Tet1^{-/-}$ mice. Pups were monitored for litter size and body weight gain. Survival rate calculation and statistical analyses were performed using Graphpad Prism software. $Tet1^{+/-}$ mice were crossed to *Lgr5-EGFP–Ires-CreERT2* mice, and $Tet1^{+/-}$; *Lgr5-EGFP–Ires-CreERT2* mice were intercrossed to generated $Tet1^{-/-}$;*Lgr5-EGFP–Ires-CreERT2* mice.

Dot blot

For the analysis of global hydroxymethylation levels, genomic DNA was isolated from mouse brains, ESCs, and small intestinal epithelia using the Allprep kit (Qiagen). dsDNAs were denatured for 10 min at 95°C and spotted onto Hybond-N^{+} nitrocellulose membranes (GE Healthcare). The membrane was blocked with CAS-Block (Thermo Fisher Scientific) followed by overnight incubation at 4°C with an anti-5hmC antibody (Active Motif). Membranes were incubated with horseradish peroxidase (HRP)-conjugated goat anti-mouse antibodies (GE Healthcare) for 30 min at room temperature and developed using the ECL^{+} prime blotting detection system (GE Healthcare).

Immunohistochemistry

Dissected mouse intestinal tissues were cut open along the longitude axis, washed in cold PBS, and fixed overnight in 4% paraformaldehyde at 4°C before paraffin-embedding. Antigen retrieval was performed using retriever in buffer A (Electron Microscopy Sciences), and tissue sections were incubated overnight at 4°C with anti-5mC (Active Motif), anti-5hmC (Active Motif), anti-Ki67 (BD Pharmingen), anti-Axin2 (Abcam), anti-Sox9 (Millipore), anti-c-Myc (Santa Cruz Biotechnology), and anti-GFP (Aves Labs) antibodies. After incubation with secondary antibodies (Vector Laboratories) for 2 h at room temperature, samples were mounted in fluorescent mounting medium (Dako) or developed using the VectaStain Elite ABC kit (Vector Laboratories). Images were acquired using a Nikon Eclipse 80i fluorescence microscope and a Leica SP8 confocal microscope.

$Lgr5^{+}$, crypt, and villus cell isolation

Small intestines were dissected and opened longitudinally. The tissues were washed in cold PBS and scraped gently on the luminal side with a glass slide to obtain villus cells. The remaining tissue was incubated with rotation in 5 mM EDTA/HBSS for 30 min at 4°C. After EDTA incubation, the tissue was vigorously shaken for 15 sec. The first fraction was villus-rich and thus discarded. After further shaking, the supernatant enriched for

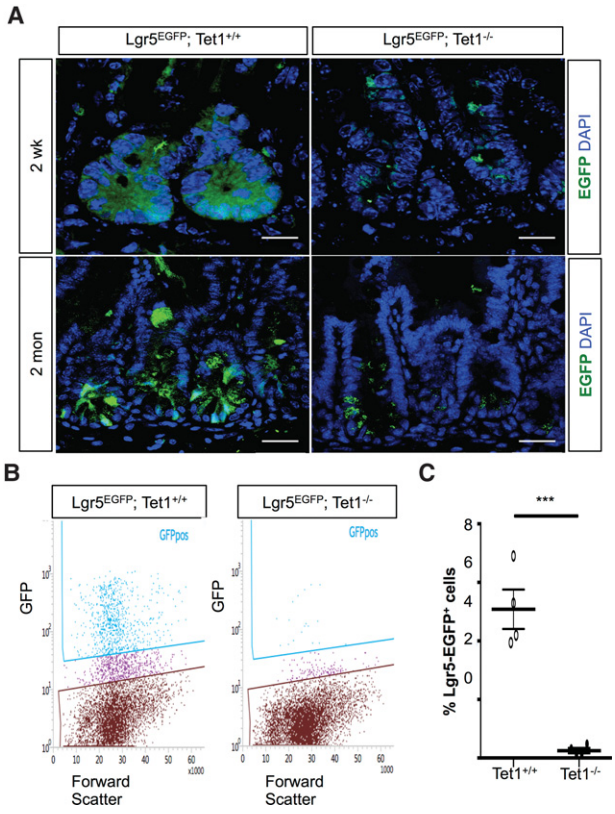

Figure 6. Reduction of Lgr5 expression in *Tet1*-null mouse intestines. (*A*) Decreased Lgr5-EGFP expression levels in 2-wk-old and 2-mo-old *Tet1*-null jejunum as detected by immunofluorescence staining of GFP (green). Bars, 20 µm. (*B*) FACS analysis demonstrates loss of Lgr5-EGFP$^+$ cells in 2-mo-old $Tet1^{-/-}$ mice. (*C*) Quantification of Lgr5-EGFP$^+$ cell number in 2-mo-old $Tet1^{+/+}$ and $Tet1^{-/-}$ mice. (***) *P*-value < 0.001. $n = 4$.

intestinal crypts was passed through a 70-µm cell strainer to remove residual villus material and was centrifuged at 600 rpm for 2 min to collect crypts. For Lgr5$^+$ cell sorting, isolated crypts were dissociated with TrypLe express (Thermo Fisher Scientific) for 20 min at 37°C and shaken every 5 min to prevent cell clumping. Dissociated cells were passed through a 40-µm cell strainer and washed with Hank's balanced salt solution (HBSS). GFP$^+$ cells were separated on a FACS Diva (BD Bioscience).

DNA (hydroxyl)methylation analysis

Genomic DNA was isolated from sorted Lgr5$^+$, crypt, and villus cells using the AllPrep kit (Qiagen) and sonicated to an average size of 150–300 base pairs (bp) (Covaris). DNA fragments were denatured for 10 min at 95°C and immunoprecipitated using 2 µL of anti-5mC (Active Motif) or anti-5hmC (Active Motif) antibody and 10 µL of Protein G beads (Thermo Fisher Scientific) in immunoprecipitation buffer (10 mM sodium phosphate at pH 7.0, 140 mM NaCl, 0.05% Triton X-100). For Me/hMeDIP-qPCR, hydroxymethylated DNA and input DNA were quantified on an Mx3005P qPCR system (Applied Biosystems) using the Brilliant II SYBR Green qPCR master mix (Agilent). qPCR primer sequences are in Supplemental Table S3. For hMeDIP-seq, DNA fragments were ligated with Illumina adaptors using the NEBNext DNA library preparation master mix set (New England Biolabs). Following adaptor ligation, DNA fragments were denatured and immunoprecipitated using an anti-5hmC antibody (Active Motif). Hydroxymethylated DNA was amplified with adapter-specific primers (12 cycles). Amplified fragments ranging from 150 to 200 bp were size-selected followed by sequencing on a HiSeq2000 (Illumina).

Mapping of sequencing data and bioinformatics

Reads were aligned to the mouse reference genome (NCBI build 37, mm9) using Bowtie (Langmead et al. 2009). Only unique reads were used for peak calling and annotation by HOMER (Heinz et al. 2010). BedGraph files were generated and viewed on the University of California at Santa Cruz Genome Browser. DhMRs were determined by comparing 5hmC peak levels in one sample with the other in each direction (fold change cutoff = 5; *P*-value cutoff = 1.00×10^{-4}). Gene ontology analysis was performed with DAVID (Huang et al. 2009). 5hmC-enriched genes in each cell population were determined by comparing the average of normalized 5hmC tag numbers in each gene promoter and body region (fold change cutoff = 1.5).

RNA isolation, qPCR, and mRNA-seq analysis

Total RNA and complementary DNA (cDNA) were prepared using the AllPrep kit (Qiagen,) and SuperScript first strand synthesis system (Thermo Fisher Scientific). qRT–PCR reactions were performed on an Mx3005P qPCR system (Applied Biosystems) using Brilliant II SYBR Green qPCR master mix (Agilent). Relative expression levels were determined using comparative Ct values after normalizing to *Tbp*. qPCR primer sequences are in Supplemental Table S2. The RNA-seq method was detailed previously (Sheaffer et al. 2014).

Intestine organoid culture

Isolated intestinal crypts were resuspended in Matrigel (Corning) and covered with standard EGF/Noggin/R-spondin medium (Sato et al. 2009). Culture medium was changed every other day.

Data access

hMeDIP-seq data generated in this study have been deposited in ArrayExpress under accession number E-MTAB-5202.

Acknowledgments

We are grateful to Dr. Chris Lengner and Dr. Maria Golson for helpful discussions and comments on the manuscript, and Tia Bernard for maintenance of the mouse colony. We thank the morphology core of the Penn Center for Molecular Studies in Digestive and Kidney Disease (P30-DK050306) for reagents and technical assistance, and the Functional Genomics Core of the Penn Diabetes Research Center (P30-DK019525) for performing sequencing and analysis. This work was funded by R37-DK053839 to K.H.K. R.K. performed experiments and wrote the manuscript draft. K.L.S., I.C., and K.-J.W. contributed data and analyses. K.H.K. conceived and directed the study and edited the manuscript.

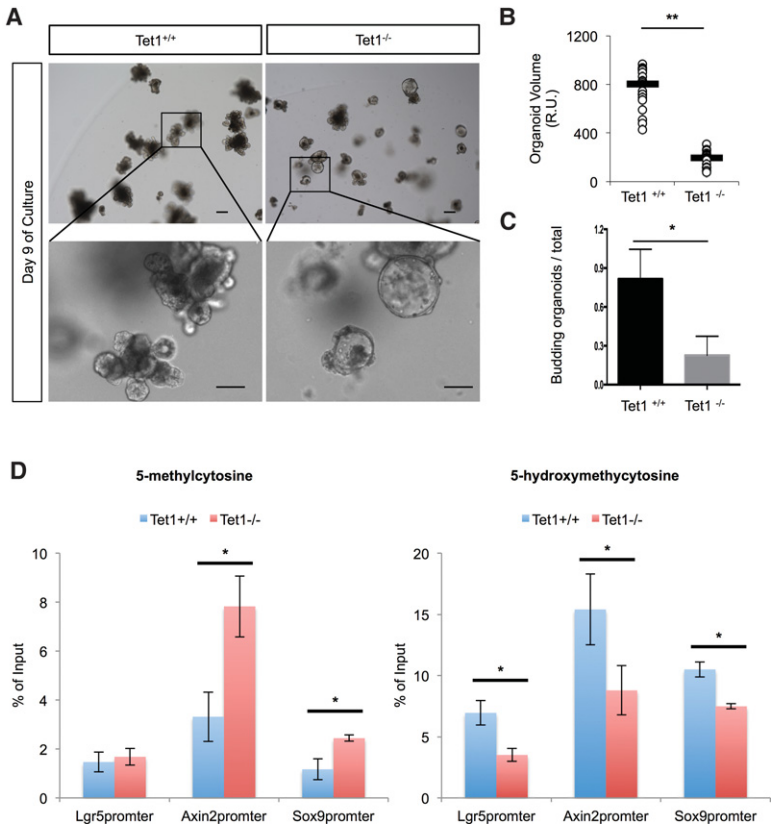

Figure 7. Budding organoid-forming potential is reduced in the absence of Tet1. (*A*) Images of intestinal organoid formation from 2-wk-old $Tet1^{+/+}$ and $Tet1^{-/-}$ jejunal crypts. Bars, 10 µm. (*B*) Quantification of intestinal organoid volume after 9 d of culture. (**) *P*-value < 0.01. $n = 3$. (*C*) Ratio of budding organoids over total organoids and spheroids. (*) *P*-value < 0.05. $n = 3$. (*D*) Differential 5mC and 5hmC levels at the promoters of Lgr5, Axin2, and Sox9 in 2-wk-old $Tet1^{+/+}$ and $Tet1^{-/-}$ crypts. (*) *P*-value < 0.05. $n = 3$.

References

Avrahami D, Li C, Zhang J, Schug J, Avrahami R, Rao S, Stadler MB, Burger L, Schübeler D, Glaser B, et al. 2015. Aging-dependent demethylation of regulatory elements correlates with chromatin state and improved β cell function. *Cell Metab* **22:** 619–632.

Barker N, van Es JH, Kuipers J, Kujala P, van den Born M, Cozijnsen M, Haegebarth A, Korving J, Begthel H, Peters PJ, et al. 2007. Identification of stem cells in small intestine and colon by marker gene *Lgr5*. *Nature* **449:** 1003–1007.

Baylin SB, Esteller M, Rountree MR, Bachman KE, Schuebel K, Herman JG. 2001. Aberrant patterns of DNA methylation, chromatin formation and gene expression in cancer. *Hum Mol Genet* **10:** 687–692.

Choi I, Kim R, Lim H-WW, Kaestner KH, Won K-JJ. 2014. 5-hydroxymethylcytosine represses the activity of enhancers in embryonic stem cells: a new epigenetic signature for gene regulation. *BMC Genomics* **15:** 670.

Cimmino L, Dawlaty MM, Ndiaye-Lobry D, Yap Y, Bakogianni S, Yu Y, Bhattacharyya S, Shaknovich R, Geng H, Lobry C, et al. 2015. TET1 is a tumor suppressor of hematopoietic malignancy. *Nat Immunol* **16:** 653–662.

Dawlaty MM, Ganz K, Powell BE, Hu Y-CC, Markoulaki S, Cheng AW, Gao Q, Kim J, Choi S-WW, Page DC, et al. 2011. Tet1 is dispensable for maintaining pluripotency and its loss is compatible with embryonic and postnatal development. *Cell Stem Cell* **9:** 166–175.

Elliott EN, Sheaffer KL, Schug J, Stappenbeck TS, Kaestner KH. 2015. Dnmt1 is essential to maintain progenitors in the perinatal intestinal epithelium. *Development* **142:** 2163–2172.

Elliott EN, Sheaffer KL, Kaestner KH. 2016. The 'de novo' DNA methyltransferase Dnmt3b compensates the Dnmt1-deficient intestinal epithelium. *Elife* **5**.

Esteller M. 2007. Cancer epigenomics: DNA methylomes and histone-modification maps. *Nat Rev Genet* **8:** 286–298.

Fordham RP, Yui S, Hannan N, Soendergaard C, Madgwick A, Schweiger PJ, Nielsen OH, Vallier L, Pedersen RA, Nakamura T, et al. 2013. Transplantation of expanded fetal intestinal progenitors contributes to colon regeneration after injury. *Cell Stem Cell* **13:** 734–744.

Gregorieff A, Clevers H. 2005. Wnt signaling in the intestinal epithelium: from endoderm to cancer. *Genes Dev* **19:** 877–890.

Hahn MA, Qiu R, Wu X, Li AX, Zhang H, Wang J, Jui J, Jin S-GG, Jiang Y, Pfeifer GP, et al. 2013. Dynamics of 5-hydroxymethylcytosine and chromatin marks in Mammalian neurogenesis. *Cell Rep* **3:** 291–300.

Heinz S, Benner C, Spann N, Bertolino E, Lin YC, Laslo P, Cheng JX, Murre C, Singh H, Glass CK. 2010. Simple combinations of lineage-determining transcription factors prime *cis*-regulatory elements required for macrophage and B cell identities. *Mol Cell* **38:** 576–589.

Huang DW, Sherman BT, Lempicki RA. 2009. Systematic and integrative analysis of large gene lists using DAVID bioinformatics resources. *Nat Protoc* **4:** 44–57.

Ito S, Shen L, Dai Q, Wu SC, Collins LB, Swenberg JA, He C, Zhang Y. 2011. Tet proteins can convert 5-methylcytosine to 5-formylcytosine and 5-carboxylcytosine. *Science* **333:** 1300–1303.

Jin S-GG, Jiang Y, Qiu R, Rauch TA, Wang Y, Schackert G, Krex D, Lu Q, Pfeifer GP. 2011. 5-Hydroxymethylcytosine is strongly depleted in human cancers but its levels do not correlate with IDH1 mutations. *Cancer Res* **71:** 7360–7365.

Kaaij LT, van de Wetering M, Fang F, Decato B, Molaro A, van de Werken HJ, van Es JH, Schuijers J, de Wit E, de Laat W, et al. 2013. DNA methylation dynamics during intestinal stem cell differentiation reveals enhancers driving gene expression in the villus. *Genome Biol* **14:** R50.

Kang J, Lienhard M, Pastor WA, Chawla A, Novotny M, Tsagaratou A, Lasken RS, Thompson EC, Surani MA, Koralov SB, et al. 2015. Simultaneous deletion of the methylcytosine oxidases Tet1 and Tet3 increases transcriptome variability in early embryogenesis. *Proc Natl Acad Sci* **112:** 45.

Kim T-HH, Escudero S, Shivdasani RA. 2012. Intact function of Lgr5 receptor-expressing intestinal stem cells in the absence of Paneth cells. *Proc Natl Acad Sci* **109:** 3932–3937.

Kinzel B, Pikiolek M, Orsini V, Sprunger J, Isken A, Zietzling S, Desplanches M, Dubost V, Breustedt D, Valdez R, et al. 2014. Functional roles of Lgr4 and Lgr5 in embryonic gut, kidney and skin development in mice. *Dev Biol* **390:** 181–190.

Kriaucionis S, Heintz N. 2009. The nuclear DNA base 5-hydroxymethylcytosine is present in Purkinje neurons and the brain. *Science* **324:** 929–930.

Langmead B, Trapnell C, Pop M, Salzberg SL. 2009. Ultrafast and memory-efficient alignment of short DNA sequences to the human genome. *Genome Biol* **10:** R25.

Li E, Bestor TH, Jaenisch R. 1992. Targeted mutation of the DNA methyltransferase gene results in embryonic lethality. *Cell* **69:** 915–926.

Lian CG, Xu Y, Ceol C, Wu F, Larson A, Dresser K, Xu W, Tan L, Hu Y, Zhan Q, et al. 2012. Loss of 5-hydroxymethylcytosine is an epigenetic hallmark of melanoma. *Cell* **150:** 1135–1146.

Maiti A, Drohat AC. 2011. Thymine DNA glycosylase can rapidly excise 5-formylcytosine and 5-carboxylcytosine potential implications for active demethylation of CpG sites. *J Biol Chem* **286:** 35334–35338.

Mustata RC, Vasile G, Fernandez-Vallone V, Strollo S, Lefort A, Libert F, Monteyne D, Pérez-Morga D, Vassart G, Garcia M-I. 2013. Identification of Lgr5-independent spheroid-generating progenitors of the mouse fetal intestinal epithelium. *Cell Rep* **5:** 421–432.

Okano M, Bell DW, Haber DA, Li E. 1999. DNA methyltransferases Dnmt3a and Dnmt3b are essential for de novo methylation and mammalian development. *Cell* **99:** 247–257.

Pastor WA, Pape UJ, Huang Y, Henderson HR, Lister R, Ko M, McLoughlin EM, Brudno Y, Mahapatra S, Kapranov P, et al. 2011. Genome-wide mapping of 5-hydroxymethylcytosine in embryonic stem cells. *Nature* **473:** 394–397.

Rao JN, Wang J-YY. 2010. *Regulation of gastrointestinal mucosal growth*. Morgan & Claypool Publishers. San Rafael, CA.

Reik W, Dean W, Walter J. 2001. Epigenetic reprogramming in mammalian development. *Science* **293:** 1089–1093.

Rudenko A, Dawlaty MM, Seo J, Cheng AW, Meng J, Le T, Faull KF, Jaenisch R, Tsai L-HH. 2013. Tet1 is critical for neuronal activity-regulated gene expression and memory extinction. *Neuron* **79:** 1109–1122.

Sato T, Vries RG, Snippert HJ, van de Wetering M, Barker N, Stange DE, van Es JH, Abo A, Kujala P, Peters PJ, et al. 2009. Single Lgr5 stem cells build crypt-villus structures in vitro without a mesenchymal niche. *Nature* **459:** 262–265.

Sheaffer KL, Kim R, Aoki R, Elliott EN, Schug J, Burger L, Schübeler D, Kaestner KH. 2014. DNA methylation is required for the control of stem cell differentiation in the small intestine. *Genes Dev* **28:** 652–664.

Smith ZD, Meissner A. 2013. DNA methylation: roles in mammalian development. *Nat Rev Genet* **14:** 204–220.

Tahiliani M, Koh KP, Shen Y, Pastor WA, Bandukwala H, Brudno Y, Agarwal S, Iyer LM, Liu DR, Aravind L, et al. 2009. Conversion of 5-methylcytosine to 5-hydroxymethylcytosine in mammalian DNA by MLL partner TET1. *Science* **324:** 930–935.

Weber AR, Krawczyk C, Robertson AB, Kuśnierczyk A, Vågbø CB, Schuermann D, Klungland A, Schär P. 2016. Biochemical reconstitution of TET1–TDG–BER-dependent active DNA demethylation reveals a highly coordinated mechanism. *Nat Commun* **7:** 10806.

Wu H, D'Alessio AC, Ito S, Wang Z, Cui K, Zhao K, Sun YE, Zhang Y. 2011. Genome-wide analysis of 5-hydroxymethylcytosine distribution reveals its dual function in transcriptional regulation in mouse embryonic stem cells. *Genes Dev* **25:** 679–684.

Xin Y-JJ, Yuan B, Yu B, Wang Y-QQ, Wu J-JJ, Zhou W-HH, Qiu Z. 2015. Tet1-mediated DNA demethylation regulates neuronal cell death induced by oxidative stress. *Sci Rep* **5:** 7645.

Yu D-HH, Gadkari M, Zhou Q, Yu S, Gao N, Guan Y, Schady D, Roshan TN, Chen M-HH, Laritsky E, et al. 2015. Postnatal epigenetic regulation of intestinal stem cells requires DNA methylation and is guided by the microbiome. *Genome Biol* **16:** 211.

Zhang R-RR, Cui Q-YY, Murai K, Lim YC, Smith ZD, Jin S, Ye P, Rosa L, Lee YK, Wu H-PP, et al. 2013. Tet1 regulates adult hippocampal neurogenesis and cognition. *Cell Stem Cell* **13:** 237–245.